Characterizing Spatial Resolution of a Fringe Projection System for Measuring Additively Manufactured Surfaces

Bin Zhang[1], Angela Davies[1], John Ziegert[2], and Christopher Evans[2]
[1]Department of Physics and Optical Science
The University of North Carolina at Charlotte,
Charlotte, NC, USA
[2]Department of Mechanical Engineering and Engineering Science
The University of North Carolina at Charlotte,
Charlotte, NC, USA

INTRODUCTION

One of the biggest challenges for metal additive manufacturing is the inability to control surface quality. An approach to solve this problem is to use in-situ metrology systems. Fast data acquisition and a relatively long working distance make fringe projection a viable solution for in-situ metrology of layered metal additive manufacturing process [1], [2]. Surfaces created by metal additive processes, particularly the laser powder bed fusion (LPBF) process, are rough, porous and textured. The roughness and texture are the results of laser scanning and are related to the process parameters such as laser power, scan velocity, and hatch distance (laser step over). The combination of the parameters creates a unique surface texture with rich spatial frequency content. Figure 1 shows such a texture with a fused square on a layer of Inconel-625 metal powder. The laser scan path is along the vertical axis with a step over of 90 µm. The laser power is 290 W, and the scan speed is 110 mm/s. The fused surface is measured in situ by a fringe projection system. The measured topography shows clear periodic structures near the bottom edge along the x-axis (Figure 1 (d)). Fourier analysis of the measured profile shows a strong peak at the spatial frequency corresponding to twice the hatch distance, suggesting a merge of two scans due to the closeness (time-wise) of the two scan paths.

The capability to resolve such detailed texture relies on the instrument's spatial resolution. One metric that characterizes the spatial resolution for a topography measuring instrument is the instrument transfer function (ITF) [3]. ITF delivers the factor by which the amplitude of a spatial frequency component drops with increasing spatial frequency.

In this paper, we study the applicability of ITF to a fringe projection system for measuring additively manufactured surfaces and provide a practical method to measure ITF using a stepped surface.

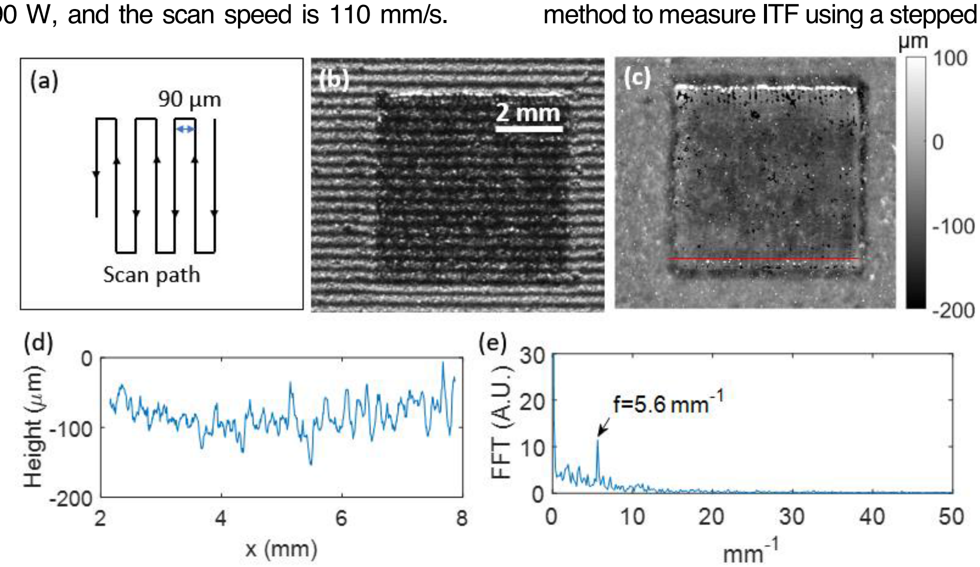

FIGURE 1. A fused square on a layer of Inconel-625 metal powder created by the LPBF process: (a) laser scan path, (b) sinusoidal fringe pattern on a fused layer of powder, (c) the height map of the fused powder layer, (d) a cross-section profile near the bottom edge of the fused region, and (d) the Fourier spectrum of the line trace.

FRINGE PROJECTION SYSTEM

The fringe projection system is developed for a LPBF machine created at the Edison Welding Institute (FIGURE). The fringe projection system consists of a commercial DLP projector (Vivitek Qumi Q5) and a machine vision camera (Point Grey Flea 3). The projector is mounted on top of the chamber, illuminating the powder bed through an AR coated glass window at a 35° angle. The camera is mounted inside the chamber, approximately 200 mm above the powder bed. To generate a high-density fringe pattern, the original projection lens is replaced with a 125-mm achromatic doublet lens and an adjustable lens tube. This lens can project an image of approximately 45 × 28 mm^2 at approximately 800 mm. The fringe pitch is 0.35 mm. The camera has a resolution of 4096 × 2160 pixels and a field of view of 28 × 15 mm, giving a pixel footprint (pixel pitch at object space) of 6.8 μm per pixel.

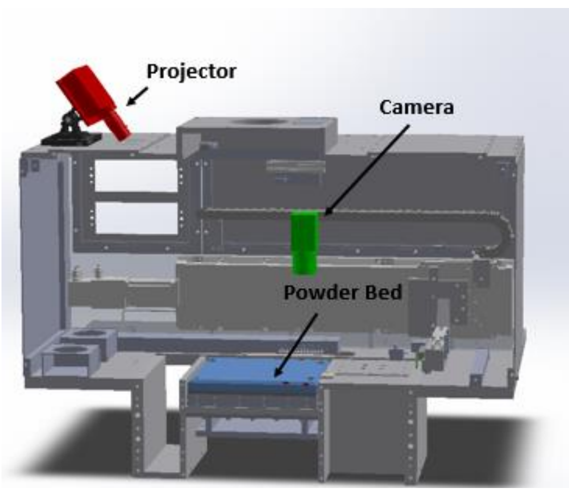

FIGURE 2. An in-situ fringe projection system for a LPBF machine (some parts are hidden for clear visualization).

The fringe projection system uses a phase shifting algorithm to measure the height variation of the object [4]. The fringe pattern is a sinusoidally-modulated gray scale image. The irradiance distribution is written as

$$I_i(x,y) = I_0\left[1+\cos\left(\frac{2\pi x}{p}+\delta_i\right)\right], \qquad (1)$$

where i indicates the ith image, I_0 is the irradiance modulation, p is the fringe pitch, and δ is the phase-shifting step size which is given by

$$\delta_i = \frac{i-1}{N}2\pi, \qquad i = 1,\ldots,N. \qquad (2)$$

where N is the total number of phase steps. A seven-step (N=7) phase shifting algorithm is chosen in this study as a balance between the number of required images and the lowest phase error. The seven captured fringe images give the wrapped phase of the surface, namely

$$\phi(x,y) = arctan\left(\frac{-\sum_{i=1}^{N}\sin(\delta_i)I_i(x,y)}{\sum_{i=1}^{N}\cos(\delta_i)I_i(x,y)}\right). \qquad (3)$$

After obtaining the wrapped phase map, a phase unwrapping algorithm is used to unfold the wrapped phase, which lies in the range from -π to π, to an extended range. Next, the carrier phase is removed from the unwrapped phase map by fitting it to Legendre polynomials. Finally, the remaining phase map is converted to the height map using a pre-calibrated system parameter called the effective wavelength. Details of these procedures can be found in our previous paper [5]. The relation between the height map and the remaining phase map is written as

$$z(x,y) = \lambda_{eff}(x,y)\cdot\phi(x,y), \qquad (4)$$

where $z(x,y)$ is the height map of the measured surface, and $\lambda_{eff}(x,y)$ is the effective wavelength map.

INSTRUMENT TRANSFER FUNCTION

The foundation of an ITF analysis is the linear theory, i.e. for a linear system, the output $g(x)$ can be expressed as the convolution of the input $f(x)$ and the system impulse response $h(x)$, namely

$$g(x) = f(x)\otimes h(x). \qquad (5)$$

In the spatial frequency domain, it is written as

$$G(f) = F(f)\cdot H(f), \qquad (6)$$

where $G(f)$, $F(f)$ and $H(f)$ are the Fourier transform of $g(x)$, $f(x)$ and $h(x)$, respectively. For an input being a height map, the function $H(f)$ is called the ITF. Thus, ITF is the ratio of the Fourier transform of the measured surface to the Fourier transform of the true surface. namely

$$H(f) = \frac{G(f)}{F(f)}. \qquad (7)$$

To characterize an instrument with an ITF, the instrument must be justified as a linear system. A linear system can be determined by the superposition property in the linear theory, i.e. the output of the sum of several inputs equals to the sum of the output of each individual input. In other words, the system must be surface independent. We show the fringe projection system satisfies this property when certain conditions are met [6]. Specifically, a fringe projection system can be approximated as a linear system when two conditions are met: 1) the amplitude of each spatial frequency component of the surface is much smaller than the effective wavelength, and 2) the width of the point spread function of the camera (25 μm) is much smaller than the effective wavelength (0.5 mm). The first condition states that the linearity is related to the amplitude of the surface. To draw a linearity boundary for a measured surface, we calculate the ITF from the simulations of fringe projection measurements of sinusoidal surfaces. The ITF does not change until the amplitude of the sinusoidal surface reaches to a limit, suggesting the linearity region is under a maximum amplitude at that spatial frequency. We define the linearity limit as the amplitude at which the ITF changes by 1%. Figure 3 shows this surface amplitude limit over a spatial frequency range between 1 to 100 cycles/mm.

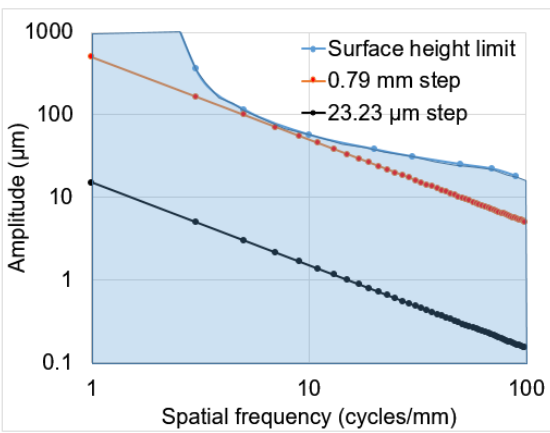

FIGURE 3. The surface height limit defines the maximum amplitude for each spatial frequency component of a measured surface for the system to behave approximately linear. A 23-μm stepped surface is below the linearity limit.

To measure the ITF experimentally, we need a test specimen which satisfy two needs: 1) it contains spatial frequency from 0 to an expected cut-off frequency, and 2) the amplitude of each spatial frequency component is smaller than the linearity limit. A stepped surface satisfies these criteria. A stepped surface contains infinite spatial frequency components; each component has an amplitude inversely proportional to its spatial frequency. The step height determines the amplitude of each spatial frequency component, which can be calculated through a Fourier analysis. A stepped surface with a step height below 0.79 mm is within the linear region (see Figure 3). A 23.23-μm step height standard is available in the lab, and is used to measure the ITF.

Conventionally, the ITF is calculated as the ratio of the Fourier transform of the measured step surface to a mathematically perfect step surface, or equivalently the ratio of the square roots of the power spectral density (PSD) functions of the measured and the mathematically perfect step surfaces [7]. In this method, a windowing process is usually used because the boundary of a step is not continuous. The windowing will cause loss of spatial frequency content. A better way to circumvent this problem is to duplicate and fold the step profile to create an artificial double-sided step profile, and to calculate the ITF with the double-sided step profiles.

Measurement of the ITF starts with measuring the stepped surface (VSLI 23.23 μm). The challenge of measuring this surface is the specular surface finish, meaning the scattered light is weak. This causes a low signal-to-noise ratio in the measured topography. Figure 4 shows a fringe pattern on the stepped surface and the height map of the stepped region outlined in red. Even with the highest illumination setting for the projector and a long exposure time (30 seconds) for the camera, the fringe visibility is still very low, leading to noise in the measured height map. The measurement noise can be reduced by averaging many line traces across the edge, but this requires alignment of the line traces with respect to the step edge. This process is similar to the slanted knife edge technique [8]. Figure 5 (a) shows the superimposed step profiles where each line trace is aligned at the step edge. The combined 1-D step profile has a much higher data density; thus, the measurement noise can be reduced by resampling the data. Since the Nyquist sampling rate (106 cycles/mm) is already higher than the camera cut-off frequency (95 cycles/mm), there is no need to oversample the step profile. Thus, we chose a sampling interval equal to the pixel pitch, namely 4.7 μm. The sampling interval is marked by the vertical lines in Figure 5 (a). The height and the x position values are averaged in each sampling interval, and the averaged step profile is shown in Figure 5 (b).

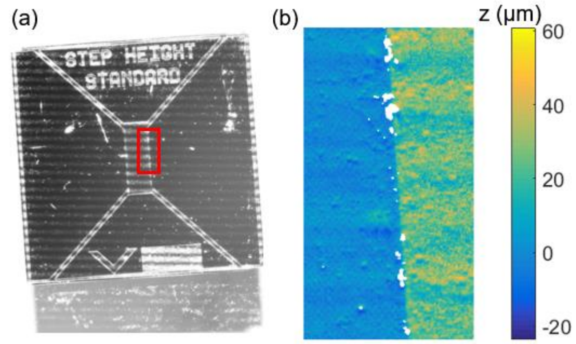

FIGURE 4. Measuring a 23-μm stepped surface with fringe projection: (a) the fringe pattern on the stepped surface, and (b) the measured height map of the outlined region.

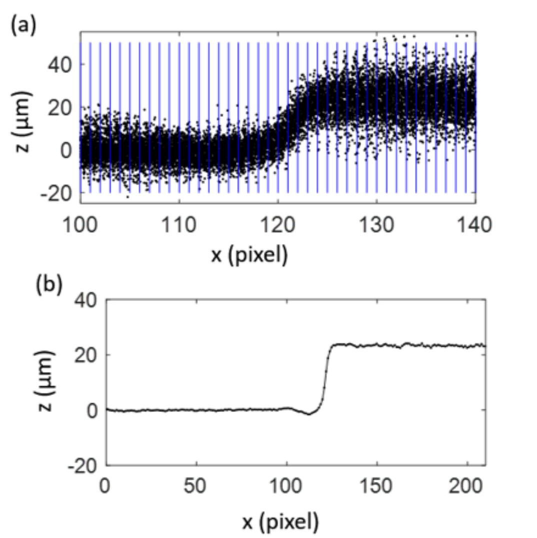

FIGURE 5. Resampling the slanted stepped surface: (a) superimposed step profiles where each profile is aligned along the step edge; the vertical lines show the sampling intervals. (b) The averaged step profile.

The noise on the upper and lower surfaces of the step has been greatly reduced after the resampling, but it is still not enough for a reasonable ITF. Even using the averaged line traces, the noise is not negligible. This causes large errors on the resultant ITF curve. Since ITF is only related to the transition between the lower and the upper surfaces of a step, the noise on the surfaces can be suppressed and this process shouldn't affect the ITF calculation. Thus, we can further reduce the noise by multiplying a noise suppression ratio of 0.1 to the two surface regions outlined in red in Figure 6 (a). Since the transition region is visually determined, it can introduce uncertainty to the ITF result. To evaluate this uncertainty, the window size is varied slightly from the visually determined windows, and the deviation in the ITF is added to the total uncertainty of the measured ITF. The boundary discontinuity issue is circumvented by duplicating and folding the step profile to form a double-sided step profile (Figure 6 (b)). The ITF is calculated by dividing the measured step profile by the mathematically perfect profile. To evaluate the measurement uncertainty, the stepped surface is measured 10 times, and ten ITFs are calculated. The average of the ten ITFs is shown in Figure 7.

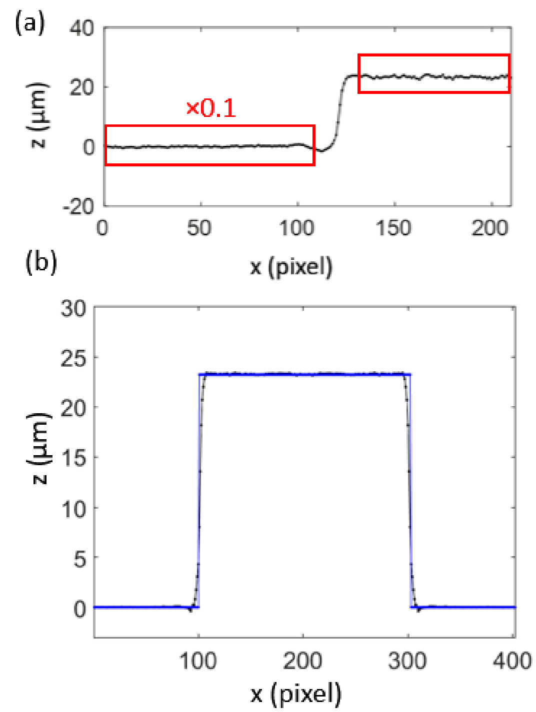

FIGURE 6. Further noise reduction on the averaged step profile: (a) The noise on the lower and upper surfaces are reduced by multiplying by a small coefficient. (b) The measured step profile (black) and the mathematically perfect step profile (blue) are duplicated and folded to form double-sided step profiles.

The total uncertainty of the measured ITF includes the repeatability, the uncertainty of choosing the step transition region, the uncertainty of choosing the noise suppression ratio and the uncertainty of finding the step angle (see Figure 7). To validate the measured ITF curve, a prediction of the ITF curve is generated through simulation using the measured MTF curve. A 2D PSF is created from the measured MTF by assuming the PSF is circularly symmetric, and the convolution of the irradiance map and the PSF is calculated. The uncertainty of the ITF prediction is also calculated, and it considers the inability of imaging the step at the best focal plane.

This uncertainty is the deviation of the predicted ITF curve caused by a PSF defocus of ±0.5 mm. This number equals to the range over which the paraxial blur spot is no bigger than the airy disk of the system. Comparison between the ITF measurement and the ITF prediction reveals that the ITF measurement is valid. The measured ITF curve falls on the lower bound of the ITF prediction band suggesting some defocus exists in the stepped surface measurements.

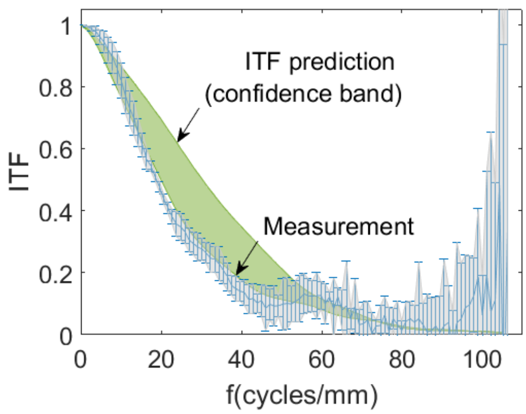

FIGURE 7. The measured ITF compared with a theoretical ITF prediction.

CONCLUSIONS

Measurements of rough and textured surfaces created by an addtive processe require the instrument to have adequate spatial resolution. The spatial resolution can be characterized by the ITF, but the instrument must be linear. We found a fringe projection system can be approximated as a linear system under two conditions: 1) the relative height of the surface is much smaller than the working distance of the camera, and 2) the amplitudes of sinusoidal components of the surface are under the linearity limit. We also measured the ITF of a fringe projection system with an appropriate stepped surface. The measurement results are compared with a predicted ITF (confidence band) calculated through simulations. The comparison shows that the measured ITF agrees with the ITF prediction.

ACKNOWLEDGEMENT

This work is partially supported by Edison Welding Institute, American Makes, National Institute of Standards and Technology, and North Carolina Research Opportunity Initiatives.

REFERENCES

[1] B. Zhang, J. Ziegert, F. Farahi, and A. Davies, "In situ surface topography of laser powder bed fusion using fringe projection," *Addit. Manuf.*, vol. 12, pp. 100–107, 2016.

[2] B. Zhang, J. Ziegert, and A. Davies, "In Situ Surface Metrology of Laser Powder Bed Fusion Processes Using Fringe Projection 2 Department of Mechanical Engineering and Engineering Science," in *Proceedings ASPE 2016 Summer Topical Meeting*, 2016, no. 1.

[3] P. de Groot, X. C. De Lega, and X. C. de Lega, "Interpreting interferometric height measurements using the instrument transfer function," *Fringe 2005*, vol. 2005, pp. 30–37, 2006.

[4] S. S. Gorthi and P. Rastogi, "Fringe projection techniques: Whither we are?," *Opt. Lasers Eng.*, vol. 48, no. 2, pp. 133–140, Feb. 2010.

[5] W. S. Land, B. Zhang, J. Ziegert, and A. Davies, "In-Situ Metrology System for Laser Powder Bed Fusion Additive Process," *Procedia Manuf.*, vol. 1, pp. 393–403, 2015.

[6] B. Zhang, A. Davies, J. Ziegert, and C. Evans, "Application of instrument transfer function to a fringe projection system for measuring rough surfaces," in *SPIE Proceedings Optics+Photonics*, 2017.

[7] C. R. Wolfe, J. D. Downie, and J. K. Lawson, "Measuring the spatial frequency transfer function of phase-measuring interferometers for laser optics," in *Proceedings of SPIE*, 1996, vol. 2870, pp. 553–557.

[8] P. D. Burns, "Slanted-Edge MTF for Digital Camera and Scanner Analysis," *Burns*, vol. 3, pp. 135–138, 2000.